Comparison of cosmological models using standard rulers and candles

Xiao-Lei Li[1], Shuo Cao[1*], Xiao-Gang Zheng[1], Song Li[2] and Marek Biesiada[1,3]

[1] Department of Astronomy, Beijing Normal University, Beijing 100875, China; *caoshuo@bnu.edu.cn*
[2] Department of Physics, Capital Normal University, Beijing 100048, China
[3] Department of Astrophysics and Cosmology, Institute of Physics, University of Silesia, Uniwersytecka 4, 40-007 Katowice, Poland

Abstract In this paper, we used standard rulers and standard candles (separately and jointly) to explore five popular dark energy models under the assumption of the spatial flatness of the Universe. As standard rulers, we used a data set comprised of 118 galactic scale strong lensing systems (individual standard rulers if properly calibrated for the mass density profile) combined with BAO diagnostics (statistical standard ruler). Type Ia supernovae served as standard candles. Unlike most previous statistical studies involving strong lensing systems, we relaxed the assumption of a singular isothermal sphere (SIS) in favor of its generalization: the power-law mass density profile. Therefore, along with cosmological model parameters, we fitted the power law index and its first derivative with respect to the redshift (thus allowing for mass density profile evolution). It turned out that the best fitted γ parameters are in agreement with each other, irrespective of the cosmological model considered. This demonstrates that galactic strong lensing systems may provide a complementary probe to test the properties of dark energy. The fits for cosmological model parameters which we obtained are in agreement with alternative studies performed by other researchers. Because standard rulers and standard candles have different parameter degeneracies, a combination of standard rulers and standard candles gives much more restrictive results for cosmological parameters. Finally, we attempted an analysis based on model selection using information theoretic criteria (AIC and BIC). Our results support the claim that the cosmological constant model is still best and there is no (at least statistical) reason to prefer any other more complex model.

Key words: (cosmology:) dark energy — cosmology: observations — (cosmology:) cosmological parameters

1 INTRODUCTION

One of the most important issues in modern cosmology is the accelerated expansion of the Universe, as deduced from Type Ia supernovae (SNe Ia) (Riess et al. 1998; Perlmutter et al. 1999) and also confirmed by other independent probes, such as Cosmic Microwave Background (CMB) (Pope et al. 2004) and Large Scale Structure (LSS) studies (Spergel et al. 2003). In order to explain this phenomenon, a new component, called dark energy, which fuels the cosmic acceleration due to its negative pressure and may dominate the Universe at late times, has been introduced.

Although the cosmological constant Λ (Peebles & Ratra 2003), the simplest candidate for dark energy, seems to agree with current observations, it suffers from the well-known fine tuning and coincidence problems. Therefore, a variety of dark energy models, including different dark energy equation of state (EoS) parametrizations such as the XCDM model (Ratra & Peebles 1988), and Chevalier-Polarski-Linder (CPL) model (Chevallier & Polarski 2001; Linder 2003), have been put forward, each of which has its own advantages and problems in explaining the acceleration of the Universe. Yet, the nature of dark energy still remains unknown. It might also be possible that observed accelerated expansion of the Universe is due to departures of the true theory of gravity from General Relativity, e.g. due to the quantum nature of gravity or possible multidimensionality of the world. Hence models such as Dvali-Gabadadze-Porrati (DGP), inspired by brane theory or Ricci Dark Energy (RDE) inspired by the holographic principle, have been proposed. Having no clear preference from the side of theory and in order to learn more about dark energy, we have to turn to the sequential upgrading of observational fits of quantities which parametrize the unknown properties of dark energy (such as density parameters or coefficients in the cosmic EoS) and seek coherence among alternative tests. In this paper we highlight the usefulness of strong lensing systems to assess the parameters of several popular dark energy models.

Because strong lensing systems are sensitive to angular diameter distance, we supplement our analysis with Baryon Acoustic Oscillation (BAO) data and compare our results with the inference made using luminosity distances measured with SNe Ia.

Strong gravitational lensing has recently developed into a serious technique in extragalactic astronomy (galactic structure studies) and in cosmology. First of all, the angular separation between images (determined by the Einstein radius of the lens) can be used to constrain and model the mass distribution of the lens (Narayan & Bartelmann 1996). Second, the time delays between images are additional sources of constraints on the mass distribution of the lens. Strong lensing time delays have recently developed into a promising new technique to constrain cosmological parameters – beginning with the Hubble constant (Suyu et al. 2010). Finally, strong lensing systems are becoming an important tool in cosmology. Earlier attempts to use such systems to constrain cosmological parameters were based on comparison between theoretical (depending on the cosmological model) and empirical distributions of image separations (Chae et al. 2002; Cao & Zhu 2012) or lens redshifts (Ofek et al. 2003; Cao et al. 2012a) in observed samples of lenses. Another approach is based on the fact that image separations in the system depend on angular diameter distances to the lens and to the source, which in turn are determined by background cosmology. This method applied in the context of dark energy was first proposed in the papers of Futamase & Yoshida (2001); Biesiada (2006); Gilmore & Natarajan (2009) and has been further developed in recent works (Biesiada et al. 2010; Cao et al. 2012b).

However, there are two well known challenges to using this method as a cosmological probe. The first issue is that the detailed mass distribution of the lens and its possible evolution in time are not clear enough. The second challenge is the limited number of observed gravitational lensing systems with complete spectroscopic and astrometric information necessary for this technique. It is only quite recently that reasonable catalogs of strong lensing systems have started to become available. In this paper, we use an approach proposed by Cao et al. (2015a) where the lensing galaxy is assumed to have a spherically symmetric mass distribution described by the power-law slope factor which is allowed to evolve with redshift.

BAO and strong lensing systems together constitute such independent standard rulers which may have different degeneracies in the parameter space of dark energy models (Biesiada et al. 2011). Moreover, we also take SNe Ia for comparison as an independent probe (standard candles).

The details of the method we used and the data set are shown in Section 2. In Section 3, we present cosmological models considered and the corresponding results. In order to compare dark energy models with different numbers of parameters and decide which model is preferred by the current data, in Section 4 we apply two model selection techniques, i.e. Akaike Information Criterion (AIC)

and Bayesian Information Criterion (BIC). Finally the results are summarized in Section 5.

2 METHOD AND DATA

2.1 Strong Lensing Systems

A strong lensing system with the intervening galaxy acting as a lens usually produces multiple images of the source. Image separation depends in the first place on the mass of the lens (suitably parametrized by stellar velocity dispersion) but also on the angular diameter distances between the lens and the source and between the observer and the lens. The angular diameter distance between two objects at redshifts z_1 and z_2 respectively is determined by background cosmology

$$D(z_1, z_2; \boldsymbol{p}) = \frac{c}{H_0(1 + z_2)} \int_{z_1}^{z_2} \frac{dz}{E(z; \boldsymbol{p})}, \quad (1)$$

where $E(z; \boldsymbol{p}) = H(z; \boldsymbol{p})/H_0$ is the dimensionless expansion rate, H_0 is the Hubble constant and $\boldsymbol{p}$ denotes the parameters of a particular cosmological model considered.

Under the assumption of the singular isothermal sphere (SIS) model, which is currently a standard description for elliptical galaxies acting as lenses, the Einstein radius θ_E is given by

$$\theta_E = 4\pi \frac{D_{ls}}{D_s} \frac{\sigma_{SIS}^2}{c^2}, \quad (2)$$

where D_{ls} and D_s are angular diameter distances between a lensing galaxy and the source and between the observer and the source, respectively. If the Einstein radius and the velocity dispersion of a lensing galaxy are known from observations, then the ratio of angular diameter distances D_{ls}/D_s can be obtained from Equation (2). The main challenge here is how to get the velocity dispersion of the lensing galaxy σ_{SIS} (which is the SIS model parameter) from central stellar velocity dispersion σ_0 obtained from spectroscopy. Previous analysis using strong gravitational lensing systems took the phenomenological approach to relate these two velocity dispersions through $\sigma_{SIS} = f_E \sigma_0$, where f_E was a free parameter with $0.8 < f_E^2 < 1.2$ (Ofek et al. 2003; Cao et al. 2012b).

In this paper, we generalize the SIS model to a spherically symmetric power-law mass distribution $\rho \sim r^{-\gamma}$ (Cao et al. 2015a). Accordingly, the Einstein radius can be rewritten as

$$\theta_E = 4\pi \frac{D_{ls}}{D_s} \frac{\sigma_{ap}^2}{c^2} \left(\frac{\theta_E}{\theta_{ap}} \right)^{2-\gamma} f(\gamma), \quad (3)$$

where σ_{ap} is the velocity dispersion inside an aperture with size θ_{ap}, and

$$f(\gamma) = -\frac{1}{\sqrt{\pi}} \frac{(5 - 2\gamma)(1 - \gamma)}{3 - \gamma} \frac{\Gamma(\gamma - 1)}{\Gamma(\gamma - \frac{2}{3})} \left[\frac{\Gamma(\frac{\gamma}{2}) - \frac{1}{2}}{\Gamma(\frac{\gamma}{2})} \right]^2. \quad (4)$$

As a result, the observational value of the angular diameter distance ratio reads

$$D^{\mathrm{obs}} = \frac{D_{\mathrm{ls}}}{D_{\mathrm{s}}} = \frac{c^2\theta_{\mathrm{E}}}{4\pi\sigma_{\mathrm{ap}}^2}\left(\frac{\theta_{\mathrm{ap}}}{\theta_{\mathrm{E}}}\right)^{2-\gamma} f^{-1}(\gamma), \qquad (5)$$

and its theoretical counterpart can be obtained from Equation (1)

$$D^{\mathrm{th}}(z_1, z_{\mathrm{s}}; \boldsymbol{p}) = \frac{D_{\mathrm{ls}}(\boldsymbol{p})}{D_{\mathrm{s}}(\boldsymbol{p})} = \frac{\int_{z_1}^{z_{\mathrm{s}}} \frac{dz}{E(z;\boldsymbol{p})}}{\int_0^{z_{\mathrm{s}}} \frac{dz}{E(z;\boldsymbol{p})}}. \qquad (6)$$

One can then constrain cosmological models by minimizing the χ^2 function given by

$$\chi_{\mathrm{SL}}^2(\boldsymbol{p}) = \sum_{i=1}^{N}\left[\frac{D^{\mathrm{th}}(z_{1,i}, z_{\mathrm{s},i}; \boldsymbol{p}) - D^{\mathrm{obs}}(\sigma_{\mathrm{ap},i}, \theta_{\mathrm{E},i}; \gamma)}{\sigma_{D,i}}\right]^2, \qquad (7)$$

where the variance of D^{obs} is

$$\begin{aligned} \sigma_{D,i}^2 = &\ D^{\mathrm{obs}}(\sigma_{\mathrm{ap},i}, \theta_{\mathrm{E},i}; \gamma)^2 \\ &\times \left[4\left(\frac{\sigma_{\sigma_{\mathrm{ap}}}}{\sigma_{\mathrm{ap}}}\right)^2 + (1-\gamma)^2\left(\frac{\sigma_{\theta_{\mathrm{E}}}}{\theta_{\mathrm{E}}}\right)^2\right]. \end{aligned} \qquad (8)$$

In order to calculate σ_D, we assumed the fractional uncertainty of the Einstein radius to be at the level of 5% (i.e., $\frac{\sigma_{\theta_{\mathrm{E}}}}{\theta_{\mathrm{E}}}=0.05$) for all the lenses, and uncertainties of the velocity dispersion were taken from the data set — see Cao et al. (2015a) for details.

We treated the mass density power-law index of lensing galaxies as a free parameter to be estimated together with cosmological parameters. Moreover, since it has recently been claimed that the γ index of elliptical galaxies might have evolved with redshift (Ruff et al. 2011), we assumed the linear relation for γ: $\gamma = \gamma_0 + \gamma_1 z_1$. Furthermore, when dealing with a sample of lenses instead of a single lens system, we followed the standard practice and transformed velocity dispersion measured within the actual circular aperture to the one within a circular aperture of radius $R_{\mathrm{eff}}/2$ (half the effective radius) according to the prescription of Jorgensen et al. (1995): $\sigma_0 = \sigma_{\mathrm{ap}}(\theta_{\mathrm{eff}}/(2\theta_{\mathrm{ap}}))^{-0.04}$. This procedure has an advantage of standardizing measured velocity dispersions within the sample and introduces negligible terms to the error budget — for details see Cao et al. (2015a).

In this paper, we use a combined sample of $n = 118$ strong lensing systems from SLACS (57 lenses taken from Bolton et al. 2008; Auger et al. 2009), BELLS (25 lenses taken from Brownstein et al. (2012)), LSD (5 lenses from Treu & Koopmans 2002; Koopmans & Treu 2003; Treu & Koopmans 2004) and SL2S (31 lenses taken from Sonnenfeld et al. 2013a,b), which is the most recent compilation of galactic scale strong lensing data. This sample is compiled and summarized in table 1 of Cao et al. (2015a), in which all of the relevant information necessary to derive a cosmological model fit can be found.

2.2 Baryon Acoustic Oscillations

BAOs refer to regular, periodic fluctuations in the density of visible baryonic matter in the Universe (the LSS). Being "the statistical standard ruler" they are commonly used to investigate dark energy. From BAO observations, we used the BAO distance ratio $r_{\mathrm{s}}(z_{\mathrm{d}})/D_V(z)$ measured by the Sloan Digital Sky Survey (SDSS) Data Release 7 (DR7) (Padmanabhan et al. 2012), SDSS-III Baryon Oscillation Spectroscopic Survey (BOSS) (Anderson et al. 2012), and the clustering shown by the WiggleZ survey (Blake et al. 2012) and 6dFGS survey (Beutler et al. 2011)

$$d_z = \frac{r_{\mathrm{s}}(z_{\mathrm{d}})}{D_V(z)}. \qquad (9)$$

The meaning of the quantities $r_{\mathrm{s}}(z_{\mathrm{d}})$ and $D_V(z)$ is explained below. The effective distance is given by

$$D_V(z) \equiv \left[(1+z)^2 D_{\mathrm{A}}^2(z)\frac{cz}{H(z)}\right]^{1/3}, \qquad (10)$$

where $D_{\mathrm{A}}(z)$ is the angular diameter distance and $H(z)$ is the Hubble parameter. The comoving sound horizon scale at the baryon drag epoch is

$$r_{\mathrm{s}}(z_{\mathrm{d}}) = \int_{z_{\mathrm{d}}}^{\infty} \frac{c_{\mathrm{s}}(z')dz'}{E(z')}, \qquad (11)$$

where the speed of sound is given by the formula $c_{\mathrm{s}}(z) = 1/\sqrt{3[1 + \bar{R}_{\mathrm{b}}/(1+z)]}$ in which $\bar{R}_{\mathrm{b}} = 3\Omega_{\mathrm{b}}h^2/(4 \times 2.469 \times 10^{-5})$, and the drag epoch redshift is fitted as

$$z_{\mathrm{d}} = \frac{1291(\Omega_{\mathrm{m}}h^2)^{0.251}}{1 + 0.659(\Omega_{\mathrm{m}}h^2)^{0.828}}[1 + b_1(\Omega_{\mathrm{b}}h^2)^{b_2}], \qquad (12)$$

where $b_1 = 0.313(\Omega_{\mathrm{m}}h^2)^{-0.419}[1 + 0.607(\Omega_{\mathrm{m}}h^2)^{0.674}]$ and $b_2 = 0.238(\Omega_{\mathrm{m}}h^2)^{0.233}$.

The χ^2 function for BAO data is defined as

$$\chi_{\mathrm{BAO}}^2 = (\boldsymbol{x} - \boldsymbol{d})^T (C_{\mathrm{BAO}}^{-1})(\boldsymbol{x} - \boldsymbol{d}), \qquad (13)$$

where

$$\begin{aligned} \boldsymbol{x} - \boldsymbol{d} = &\ [r_{\mathrm{s}}/D_V(0.1) - 0.336, D_V(0.35)/r_{\mathrm{s}} - 8.88, \\ &\ D_V(0.57)/r_{\mathrm{s}} - 13.67, r_{\mathrm{s}}/D_V(0.44) - 0.0916, \\ &\ r_{\mathrm{s}}/D_V(0.60) - 0.0726, r_{\mathrm{s}}/D_V(0.73) - 0.0592] \end{aligned} \qquad (14)$$

and C_{BAO}^{-1} is the corresponding inverse covariance matrix adopted by Hinshaw et al. (2013). In order to constrain the cosmological parameters with standard rulers, i.e. strong lensing systems and BAO, we used the joint χ^2, which is defined as

$$\chi_{\mathrm{SL+BAO}}^2 = \chi_{\mathrm{SL}}^2 + \chi_{\mathrm{BAO}}^2. \qquad (15)$$

2.3 SNe Ia

Up to now, we have discussed standard rulers, but it was standard candles (SNe Ia) that kicked off the story of the accelerated expansion of the Universe. They have remained a reference point for discussions and tests of cosmological models. Because standard rulers (SL+BAO) and standard candles measure the distances based on different concepts, the cosmological inferences based on them have different degeneracies in parameter space. Therefore, we also considered constraints on cosmologies coming from SN Ia observations; for comparison and also for the sake of complementarity. In this paper, we used the latest Union2.1 compilation released by the Supernova Cosmology Project collaboration consisting of 580 SN Ia data points (Suzuki et al. 2012), taking into consideration systematic errors of the observed distance modulus (Cao & Zhu 2014). The Hubble constant H_0 was treated as a nuisance parameter and was marginalized over with a flat prior. The $\chi^2_{\rm SN}$ function for the supernova data is given by

$$\chi^2_{\rm SN} = \sum_{i,j} \alpha_i C^{-1}_{\rm SN}(z_i, z_j) \alpha_j$$
$$- \frac{[\sum_{ij} \alpha_i C^{-1}_{\rm SN}(z_i, z_j) - \ln 10/5]^2}{\sum_{ij} C^{-1}_{\rm SN}(z_i, z_j)}$$
$$-2 \ln \left(\frac{\ln 10}{5} \sqrt{\frac{2\pi}{\sum_{ij} C^{-1}_{\rm SN}(z_i, z_j)}} \right), \qquad (16)$$

where $\alpha_i = \mu_{\rm obs}(z_i) - 25 - 5 \log_{10}[H_0 D_L(z_i)/c]$ and $C_{\rm SN}(z_i, z_j)$ is the covariance matrix.

Finally, we also performed a joint analysis with both standard rulers and standard candles using the combined chi-square function

$$\chi^2_{\rm tot} = \chi^2_{\rm SL} + \chi^2_{\rm BAO} + \chi^2_{\rm SN}. \qquad (17)$$

3 COSMOLOGICAL MODELS AND RESULTS

In this section, we choose several popular dark energy models and estimate their best fitted parameters using the standard rulers (strong lensing systems and BAO), standard candles and the combination of all these cosmological probes. We also examine consistency of our findings with other independent results from the literature. Table 1 reports the Hubble function for different cosmological models considered. We report the best fit values throughout our paper, and the corresponding 1σ uncertainties (68% confidence intervals) for each class of models considered. Moreover, we assume a spatially flat Universe. The results of cosmological parameters from standard rulers (SL+BAO) are presented in Table 2.

3.1 Standard Cosmological Model

Currently, the standard cosmological model, also known as the ΛCDM model, is the simplest case with constant dark energy density present in the form of a cosmological constant Λ. This agrees very well with various observational data such as CMB anisotropies, LSS distribution (Pope et al. 2004; Riess et al. 1998), etc. Formally, one can say that the cosmic EoS here is simply $w = p/\rho = -1$.

If flatness of the FRW metric is assumed, then the only cosmological parameter of this model is $\boldsymbol{p} = \{\Omega_{\rm m}\}$. We obtain $\Omega_{\rm m} = 0.279^{+0.022}_{-0.022}$ from standard rulers (SL+BAO), $\Omega_{\rm m} = 0.301^{+0.040}_{-0.041}$ from standard candles (SNe Ia) and $\Omega_{\rm m} = 0.280^{+0.020}_{-0.020}$ from the combination of standard rulers and standard candles. The results are presented in Figure 1 and Table 2. One can see that standard rulers have considerable leverage on the joint analysis.

For comparison, it is necessary to refer to earlier results obtained with other independent measurements. By studying the peculiar velocities of galaxies, the only method sensitive exclusively to the matter density parameter, Feldman et al. (2003) obtained $\Omega_{\rm m} = 0.30^{+0.17}_{-0.17}$, a value which agrees with our joint analysis within the 1σ range. Based on the WMAP 9-year results, Hinshaw et al. (2013) gave the best-fit parameter: $\Omega_{\rm m} = 0.279 \pm 0.025$ for the flat ΛCDM model, which is in perfect agreement with our result using standard rulers. Let us note that the cosmological probe inferred from CMB anisotropy measured by WMAP is also a standard ruler — the comoving size of the acoustic horizon. This is the same ruler as used in the BAO technique, so strong consistency could be expected here. More recently, using the corrected redshift - angular size relation for a sample of quasars, Cao et al. (2015b) obtained $\Omega_{\rm m} = 0.292^{+0.065}_{-0.090}$ in the spatially flat ΛCDM cosmology, which is also in a very good agreement with our findings.

3.2 Dark Energy with Constant EoS

In this case, dark energy is described by a hydrodynamic energy-momentum tensor with a constant EoS coefficient $w = p/\rho$, which leads to cosmic acceleration whenever $w < -1/3$ (Ratra & Peebles 1988).

For standard rulers, standard candles and the combined analysis, confidence regions (corresponding to 68.3% and 95.8% confidence levels) in the ($\Omega_{\rm m}, w$) plane are shown in Figure 2, with the best-fit parameters:

$$\{\Omega_{\rm m}, w\} = \left\{ 0.282^{+0.021}_{-0.023}, -0.917^{+0.194}_{-0.188} \right\},$$
$$\{\Omega_{\rm m}, w\} = \left\{ 0.287^{+0.104}_{-0.111}, -0.917^{+0.308}_{-0.304} \right\},$$
$$\{\Omega_{\rm m}, w\} = \left\{ 0.280^{+0.018}_{-0.019}, -0.947^{+0.102}_{-0.094} \right\},$$

from SL+BAO, SN and SL+BAO+SN, respectively. As can be seen from Figure 2, standard rulers (SL+BAO) and standard candles (SNe) have different degeneracies in the parameter space. Consequently, their restrictive power is different. This fact makes the joint constraint more restrictive. Our results are in excellent agreement with the previous results obtained from the ESSENCE supernova survey team (Wood-Vasey et al. 2007) who obtained $\{\Omega_{\rm m}, w\} = \left\{ 0.274^{+0.033}_{-0.020}, -1.07 \pm +0.09 \pm -0.12 \right\}$ and the Union1

Table 1 Hubble Function for Different Cosmological Models Considered

Model	Hubble function	Cosmological parameters
ΛCDM	$H^2(z) = H_0^2[\Omega_{\rm m}(1+z)^3 + (1-\Omega_{\rm m})]$	$\Omega_{\rm m}$
XCDM	$H^2(z) = H_0^2[\Omega_{\rm m}(1+z)^3 + \Omega_\Lambda(1+z)^{3(1+w)}]$	$\Omega_{\rm m}, w$
CPL	$H^2(z) = H_0^2[\Omega_{\rm m}(1+z)^3 + \Omega_\Lambda(1+z)^{3(1+w_0+w_1)}\exp(\frac{-3w_1z}{1+z})]$	w_0, w_1
RDE	$H^2(z) = H_0^2[\frac{2\Omega_{\rm m}}{2-\beta}(1+z)^3 + (1-\frac{2\Omega_{\rm m}}{2-\beta})(1+z)^{4-2/\beta}]$	$\Omega_{\rm m}, \beta$
DGP	$H^2(z) = H_0^2[(\sqrt{\Omega_{\rm m}(1+z)^3 + \Omega_{rc}} + \sqrt{\Omega_{rc}})^2]$	$\Omega_{\rm m}$

Table 2 Best Fits for Different Cosmological Models from Standard Rulers (SL+BAO)

Model	Cosmological parameters	Mass density slope parameters
ΛCDM	$\Omega_{\rm m} = 0.279^{+0.022}_{-0.022}$	$\gamma_0 = 2.094^{+0.053}_{-0.056}, \gamma_1 = -0.053^{+0.103}_{-0.102}$
XCDM	$\Omega_{\rm m} = 0.282^{+0.021}_{-0.023}, w = -0.917^{+0.194}_{-0.188}$	$\gamma_0 = 2.088^{+0.055}_{-0.056}, \gamma_1 = -0.054^{+0.104}_{-0.102}$
CPL	$w_0 = -0.879^{+0.325}_{-0.314}, w_1 = -0.464^{+0.870}_{-0.710}$	$\gamma_0 = 2.087^{+0.055}_{-0.056}, \gamma_1 = -0.055^{+0.105}_{-0.105}$
RDE	$\Omega_{\rm m} = 0.201^{+0.017}_{-0.019}, \beta = 0.566^{+0.087}_{-0.086}$	$\gamma_0 = 2.087^{+0.052}_{-0.054}, \gamma_1 = -0.052^{+0.104}_{-0.102}$
DGP	$\Omega_{\rm m} = 0.269^{+0.014}_{-0.016}$	$\gamma_0 = 2.074^{+0.050}_{-0.051}, \gamma_1 = -0.047^{+0.101}_{-0.102}$
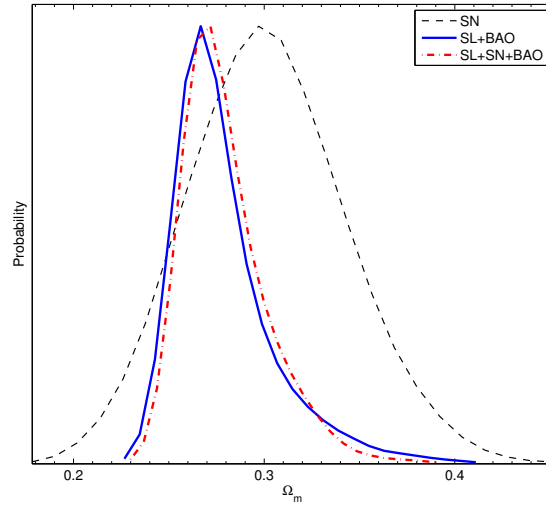
Fig. 1 Constraints on the ΛCDM model. The solid line is the result from SL+BAO, the dashed line is from SN and the dot-dashed line is from SL+BAO+SN.

SNe Ia compilation (Kowalski et al. 2008) whose results are: $\{\Omega_{\rm m}, w\} = \{0.274^{+0.033}_{-0.020}, -0.969^{+0.059+0.063}_{-0.063-0.066}\}$.

3.3 CPL Model

The constant cosmic EoS of the XCDM cosmology is only a phenomenological description, which cannot ultimately be true. Being fundamentally different from the cosmological constant, it must have some dynamical reason; e.g., in a scalar field settling down on the attractor. Therefore, one should expect that such a scalar field was evolving and left the trace of its evolution on the EoS. So, it would be natural to expect that the w coefficient varied in time, i.e. $w = w(z)$. In this paper, we take a Taylor expansion of

$w(z)$ with respect to the scale factor, which leads to the following redshift dependence: $w(z) = w_0 + w_1\frac{z}{1+z}$. This is the so called CPL model proposed in Chevallier & Polarski (2001); Linder (2003).

It has been known for some time that it is hard to get good and stringent fits for all parameters in this model. Hence, we fix the matter density parameter at the best-fit value $\Omega_{\rm m} = 0.315$ based on the recent Planck observations (Planck Collaboration et al. 2014). Our best fit values for the CPL model parameters are

$$\{w_0, w_1\} = \{-0.879^{+0.414}_{-0.431}, -0.463^{+2.108}_{-1.717}\},$$
$$\{w_0, w_1\} = \{-0.951^{+0.249}_{-0.247}, -0.4034^{+1.160}_{-1.139}\},$$
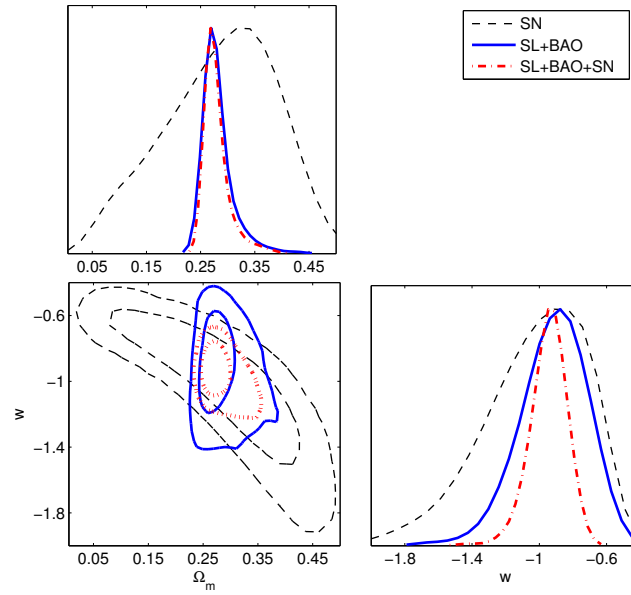$$\{w_0, w_1\} = \{-0.965^{+0.154}_{-0.155}, -0.241^{+0.498}_{-0.501}\},$$

Fig. 2 Constraints on the XCDM model. The solid line is the result from SL+BAO, the dashed line is from SN and the dot-dashed line is from SL+BAO+SN.
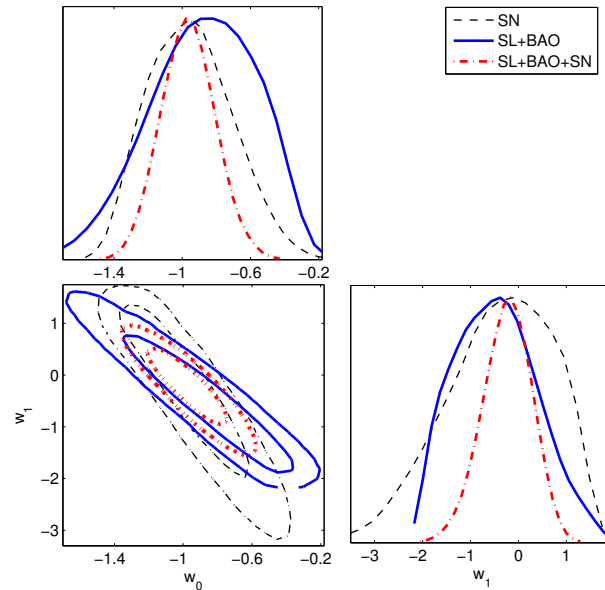

Fig. 3 Constraints on CPL parameterization with fixed $\Omega_{\mathrm{m}} = 0.315$. The solid line is the result from SL+BAO, the dashed line is from SN and the dot-dashed line is from SL+BAO+SN.

from SL+BAO, SN and SL+BAO+SN, respectively. Confidence regions (corresponding to 68.3% and 95.8% confidence levels) for standard rulers, standard candles and the combined analysis in the (w_0, w_1) plane are shown in Figure 3. One can notice that confidence contours from standard rulers and standard candles are inclined with respect to each other. This is a promising signal in light of the colinearity of w_0 and w_1 parameters (due to their fundamental anticorrelation), which has so far been a major obstacle in calculating a stronger constraint on them. This inclination gives us hope that the combined analysis will

eventually lead to a more precise assessment of w_0 and w_1 and be used to decide whether the cosmic EoS has evolved or not.

The results obtained with standard rulers turned out to correspond well with previous work by Biesiada et al. (2011), whose results (for standard rulers) were $w_0 = -0.993 \pm 0.207, w_1 = 0.609 \pm 1.071$. As far as standard candles are concerned, the result of joint analysis from WMAP+BAO+H_0+SN given by Komatsu et al. (2011) is $w_0 = -0.93 \pm 0.13, w_1 = 0.41^{+0.72}_{-0.71}$. Moreover, the combined analysis of standard rulers and candles performed in
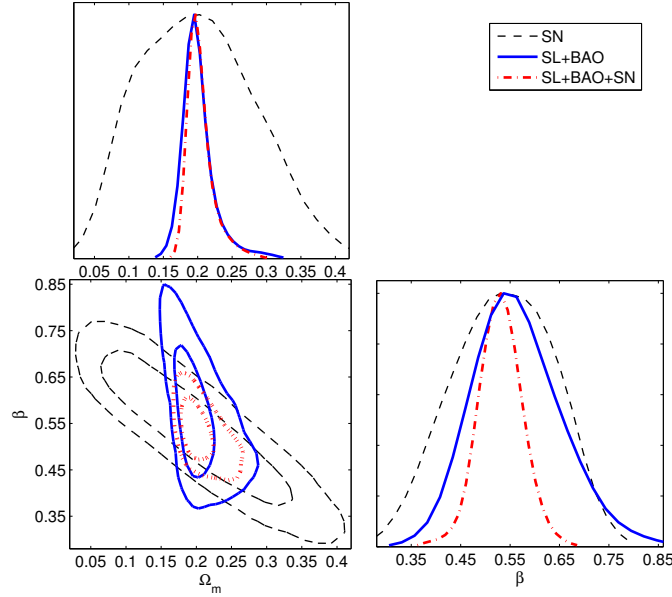
Fig. 4 Constraints on the RDE model. The solid line is the result from SL+BAO, the dashed line is from SN and the dot-dashed line is from SL+BAO+SN.
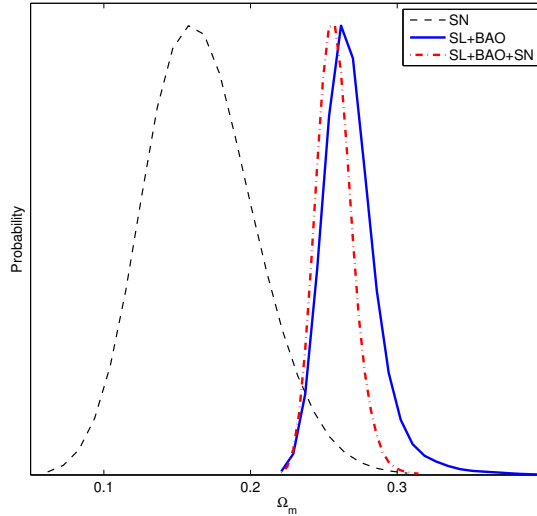

Fig. 5 Constraints on DGP. The solid line is the result from SL+BAO, the dashed line is from SN and the dot-dashed line is from SL+BAO+SN.

Biesiada et al. (2011) resulted in the following best fits: $w_0 = -0.989 \pm 0.124$, $w_1 = 0.082 \pm 0.621$. These results are in agreement with ours within 1σ. In addition, our joint analysis tends to support the models with a varying EoS which are very close to the ΛCDM model ($w_0 = -1$, $w_1 = 0$).

3.4 RDE Model

Several other cosmological models have gained a lot of attention; one of them is the so called holographic dark energy, which is inspired by the holographic principle resulting from quantum gravity. It is well known that gravita-

tional entropy of a given closed system with a characteristic length scale L is not proportional to its volume L^3, but to its surface area L^2 (Bekenstein 1981; Gao et al. 2009). Because the cosmological constant Λ scales like inverse length squared, one could postulate this length scale coinciding with the present Hubble horizon. This way, the coincidence and fine tuning problems could be alleviated. However, it turned out that this model has trouble explaining accelerated expansion of the Universe. Therefore, Gao et al. (2009) proposed to choose $|R|^{-1/2}$ as the infrared cutoff, where $R = -6(\dot{H} + 2H^2)$ is a Ricci scalar. In this section we will confront this model with data from standard rulers and standard candles. The density of dark en-

ergy in this model is

$$\rho_{\text{de}} = 3\beta M_{\text{Pl}}^2(\dot{H} + 2H^2), \quad (18)$$

where $\beta > 0$ is some constant parameter to be fitted.

With the methods described above, we obtain the following best fits for the RDE model:

$$\{\Omega_{\text{m}}, \beta\} = \{0.201_{-0.019}^{+0.017}, 0.566_{-0.086}^{+0.087}\},$$
$$\{\Omega_{\text{m}}, \beta\} = \{0.202_{-0.088}^{+0.086}, 0.534_{-0.105}^{+0.104}\},$$
$$\{\Omega_{\text{m}}, \beta\} = \{0.201_{-0.016}^{+0.016}, 0.531_{-0.041}^{+0.041}\},$$

from SL+BAO, SN and SL+BAO+SN, respectively. These results are also illustrated in Figure 4. These results are in agreement with the previous work of Cao et al. (2012a). Additionally, the best fits for different probes are very close to each other.

3.5 DGP Model

The cosmological models that we have investigated so far have been based on Einstein's theory of gravity. However, there are also other approaches which seek an explanation of accelerated expansion of the Universe by implementing modifications to General Relativity. The DGP brane world model is a well-known example of this class, based on the assumption that our 4-dimensional spacetime is embedded in a higher dimensional bulk spacetime (Dvali et al. 2000).

In this model, the Friedman equation is modified to

$$H^2 + \frac{k}{a^2} = \left[\sqrt{\frac{\rho}{3M_{\text{Pl}}^2} + \frac{1}{4r_c^2}} + \frac{1}{2r_c}\right]^2, \quad (19)$$

where $M_{\text{Pl}} = \sqrt{\frac{\hbar c}{8\pi G}}$ is the (reduced) Planck mass and $r_c = \frac{M_{\text{Pl}}^2}{2M_5^2}$ (with M_5 denoting the 5-dimensional reduced Planck mass) is the crossover scale. Introducing the Omega parameter: $\Omega_{rc} = 1/(4r_c^2 H_0^2)$, one can rewrite Equation (19) in the form leading to the Hubble function given in Table 1 (also assuming a flat Universe). The Friedman equation also leads to the normalization condition: $\Omega_k + (\sqrt{\Omega_{r_c}} + \sqrt{\Omega_{\text{m}} + \Omega_{r_c}})^2 = 1$, which simplifies to $\Omega_{r_c} = \frac{1}{4}(1 - \Omega_{\text{m}})^2$ under the assumption of a flat Universe. Therefore, the flat DGP model only contains one free parameter, Ω_{m}. The best fit values for the mass density parameter in the DGP model obtained from SL+BAO, SN and SL+BAO+SN are: $\Omega_{\text{m}} = 0.269_{-0.016}^{+0.014}$, $\Omega_{\text{m}} = 0.165_{-0.035}^{+0.036}$ and $\Omega_{\text{m}} = 0.257_{-0.012}^{+0.011}$, respectively. These results are also illustrated in Figure 5.

Former work done by Xu & Wang (2010) indicated $\Omega_{\text{m}} = 0.266_{-0.0304}^{+0.0298}$ and the results of Biesiada et al. (2011) that yielded $\Omega_{\text{m}} = 0.267 \pm 0.013$ from CMB+BAO+SL+SN match accurately with our results. Moreover, our results are in a very good agreement with Cao et al. (2012a).

Closing this section, let us stress that we have not only constrained cosmological models, but have also considered the evolution of slope factor in the mass density profile of lensing galaxies. Consequently, we also obtained the best fits for γ parameters, as shown in Table 1. It can be seen that the γ parameters estimated in different cosmological models are very similar. This suggests that the method of using distance ratios from strong lensing systems can be effective in cosmological applications. More precisely, since the γ parameters of a lens mass distribution model seem to be unaffected by the cosmological model assumed, one can hope to calibrate them within say the ΛCDM model and then use the best fits as an input for cosmological model testing with the samples like ours (118 lenses) or similar ones obtained in the future.

4 MODEL SELECTION

In the previous section, we obtained the best fits for five cosmological models from 118 galactic scale strong lensing systems combined with six BAO observations. However, the χ^2 statistic alone does not provide the most effective way to compare competing models and decide which one is preferred by the data. This question can be answered with model selection techniques (Cao et al. 2011).

Therefore, we used of two criteria: AIC (Akaike 1974) and BIC (Schwarz et al. 1978). They have became standard in applied statistics, and were first used in cosmology by Liddle (2004) and then for example by Godłowski & Szydłowski (2005) or Biesiada (2007). The value of AIC, an approximately unbiased estimator of the Kullback-Leibler divergence between the given model and the "true" one, can be calculated as

$$\text{AIC} = -2\ln L_{\text{max}} + 2k, \quad (20)$$

where L_{max} is the maximum likelihood value and k is the number of free parameters in the model. In our case, k is comprised of both cosmological parameters and galaxy mass density slopes. If the uncertainties are Gaussian, likelihood can be calculated from the chi-square function $\chi^2 = -2\ln L_{\text{max}}$. The value of AIC for a single model is meaningless in this kind of study. What is useful is the difference in values of AIC between cosmological models, ΔAIC. This difference is usually calculated with respect to the model which has the smallest value of AIC

$$\Delta\text{AIC}(i) = \text{AIC}(i) - \text{AIC}_{\text{min}}, \quad (21)$$

where the index $i = 1, ..., 5$ represents the cosmological models and $\text{AIC}_{\text{min}} = \min\{\text{AIC}(i)\}$. BIC is defined in a very similar manner to AIC, but it adds information about the sample size N

$$\text{BIC} = \chi^2 + 2k\ln N. \quad (22)$$

For the purpose of model selection, we only used the standard rulers, i.e. BAO combined with 118 lensing data. Table 3 lists the AIC and BIC values and differences for each model. One can see that both AIC and BIC criteria support ΛCDM as the best cosmological model, in light of current observational strong lensing data. Concerning the ranking of other competing models, AIC and BIC criteria

Table 3 Summary of the information criteria, AIC and BIC, for the combined SL+BAO data.

Model	AIC	ΔAIC	BIC	ΔBIC
ΛCDM	320.71	0	323.53	0
XCDM	322.61	1.89	328.25	4.71
CPL	322.77	2.06	328.41	4.88
RDE	322.59	1.88	328.23	4.63
DGP	322.76	2.05	325.58	2.05

give different conclusions. According to AIC, next are the RDE and XCDM models: the odds against them with respect to ΛCDM (see Biesiada (2007) for details) are 2.6:1 (they differ in the second decimal place). Then the CPL and DGP are supported slightly worse, with odds against being 2.8:1. In summary, one can say that besides ΛCDM as the best model, all of the other models get similar support by the standard rulers. On the other hand, BIC gives a different ranking: next after ΛCDM is the DGP brane model with odds against equal to 2.8:1. Then there are RDE (odds against being 10.1:1) and XCDM (odds against being 10.5:1) while the CPL model receives the least support with odds against being 11.5:1. In summary, one can state that BIC substantially penalizes cosmological models with more than one free parameter. In particular, our findings are in contrast with those of Biesiada (2007) who claimed that the DGP model is strongly disfavored by the data.

5 SUMMARY AND CONCLUSION

In this paper, we used standard rulers and standard candles (separately and jointly) to explore five popular dark energy models under the assumption of spatial flatness of the Universe. As standard rulers, we used a new galactic scale strong lensing data set compiled by Cao et al. (2015a) combined with BAO diagnostics. SNe Ia served as standard candles. In order to compare the degree of support given by the standard rulers to various competing dark energy models, we performed a model selection using AIC and BIC information criteria.

The main conclusions of this paper can be summarized as follows. First, by relaxing the mass density profile of the SIS model to a more general power-law density profile, the best fitted γ parameters are in agreement with each other, irrespective of the cosmological model considered. This demonstrates that inclusion of mass density power index as a free parameter does not lead to noticeable spurious effects of mixing them with cosmological parameters in the statistical procedure of fitting. Therefore, we can say that galactic strong lensing systems may provide a complementary probe to test the properties of dark energy. Second, because standard rulers and standard candles have different parameter degeneracies in cosmology, joint analysis of standard rulers and standard candles gives much more restrictive results for cosmological parameters. Third, the information theoretic criteria (AIC and BIC) support the claim that the cosmological constant model is still the best

model and there is no reason to prefer any more complex models. In light of a forthcoming new generation of sky surveys such as the EUCLID mission, Pan-STARRS, LSST and JDEM, which are expected to discover thousands to tens of thousands of strong lensing systems, it would be interesting to stay abreast of new developments. We are looking forward to seeing whether this conclusion could be changed by more gravitational lensing systems that will be observed in the future.

References

Akaike, H. 1974, IEEE Transactions on Automatic Control, 19, 716

Anderson, L., Aubourg, E., Bailey, S., et al. 2012, MNRAS, 427, 3435

Auger, M. W., Treu, T., Bolton, A. S., et al. 2009, ApJ, 705, 1099

Bekenstein, J. D. 1981, Phys. Rev. D, 23, 287

Beutler, F., Blake, C., Colless, M., et al. 2011, MNRAS, 416, 3017

Biesiada, M. 2006, Phys. Rev. D, 73, 023006

Biesiada, M. 2007, J. Cosmol. Astropart. Phys., 2, 003

Biesiada, M., Malec, B., & Piórkowska, A. 2011, RAA (Research in Astronomy and Astrophysics), 11, 641

Biesiada, M., Piórkowska, A., & Malec, B. 2010, MNRAS, 406, 1055

Blake, C., Brough, S., Colless, M., et al. 2012, MNRAS, 425, 405

Bolton, A. S., Burles, S., Koopmans, L. V. E., et al. 2008, ApJ, 682, 964

Brownstein, J. R., Bolton, A. S., Schlegel, D. J., et al. 2012, ApJ, 744, 41

Cao, S., Biesiada, M., Gavazzi, R., Piórkowska, A., & Zhu, Z.-H. 2015a, ApJ, 806, 185

Cao, S., Biesiada, M., Zheng, X., & Zhu, Z.-H. 2015b, ApJ, 806, 66

Cao, S., Covone, G., & Zhu, Z.-H. 2012a, ApJ, 755, 31

Cao, S., Pan, Y., Biesiada, M., Godlowski, W., & Zhu, Z.-H. 2012b, J. Cosmol. Astropart. Phys., 3, 016

Cao, S., & Zhu, Z.-H. 2012, A&A, 538, A43

Cao, S., & Zhu, Z.-H. 2014, Phys. Rev. D, 90, 083006

Cao, S., Zhu, Z.-H., & Zhao, R. 2011, Phys. Rev. D, 84, 023005

Chae, K.-H., Biggs, A. D., Blandford, R. D., et al. 2002, Physical Review Letters, 89, 151301

Chevallier, M., & Polarski, D. 2001, International Journal of Modern Physics D, 10, 213

Dvali, G., Gabadadze, G., & Porrati, M. 2000, Physics Letters B, 485, 208

Feldman, H., Juszkiewicz, R., Ferreira, P., et al. 2003, ApJ, 596, L131

Futamase, T., & Yoshida, S. 2001, Progress of Theoretical Physics, 105, 887

Gao, C., Wu, F., Chen, X., & Shen, Y.-G. 2009, Phys. Rev. D, 79, 043511

Gilmore, J., & Natarajan, P. 2009, MNRAS, 396, 354

Godłowski, W., & Szydłowski, M. 2005, Physics Letters B, 623, 10

Hinshaw, G., Larson, D., Komatsu, E., et al. 2013, ApJS, 208, 19

Jorgensen, I., Franx, M., & Kjaergaard, P. 1995, MNRAS, 273, 1097

Komatsu, E., Smith, K. M., Dunkley, J., et al. 2011, ApJS, 192, 18

Koopmans, L. V. E., & Treu, T. 2003, ApJ, 583, 606

Kowalski, M., Rubin, D., Aldering, G., et al. 2008, ApJ, 686, 749

Liddle, A. R. 2004, MNRAS, 351, L49

Linder, E. V. 2003, Phys. Rev. D, 68, 083503

Narayan, R., & Bartelmann, M. 1996, astro-ph/9606001

Ofek, E. O., Rix, H.-W., & Maoz, D. 2003, MNRAS, 343, 639

Padmanabhan, N., Xu, X., Eisenstein, D. J., et al. 2012, MNRAS, 427, 2132

Peebles, P. J., & Ratra, B. 2003, Reviews of Modern Physics, 75, 559

Perlmutter, S., Aldering, G., Goldhaber, G., et al. 1999, ApJ, 517, 565

Planck Collaboration, Ade, P. A. R., Aghanim, N., et al. 2014, A&A, 571, A16

Pope, A. C., Matsubara, T., Szalay, A. S., et al. 2004, ApJ, 607, 655

Ratra, B., & Peebles, P. J. E. 1988, Phys. Rev. D, 37, 3406

Riess, A. G., Filippenko, A. V., Challis, P., et al. 1998, AJ, 116, 1009

Ruff, A. J., Gavazzi, R., Marshall, P. J., et al. 2011, ApJ, 727, 96

Schwarz, G., et al. 1978, The Annals of Statistics, 6, 461

Sonnenfeld, A., Gavazzi, R., Suyu, S. H., Treu, T., & Marshall, P. J. 2013a, ApJ, 777, 97

Sonnenfeld, A., Treu, T., Gavazzi, R., et al. 2013b, ApJ, 777, 98

Spergel, D. N., Verde, L., Peiris, H. V., et al. 2003, ApJS, 148, 175

Suyu, S. H., Marshall, P. J., Auger, M. W., et al. 2010, ApJ, 711, 201

Suzuki, N., Rubin, D., Lidman, C., et al. 2012, ApJ, 746, 85

Treu, T., & Koopmans, L. V. E. 2002, ApJ, 575, 87

Treu, T., & Koopmans, L. V. E. 2004, ApJ, 611, 739

Wood-Vasey, W. M., Miknaitis, G., Stubbs, C. W., et al. 2007, ApJ, 666, 694

Xu, L., & Wang, Y. 2010, Phys. Rev. D, 82, 043503